Journal of Luminescence 134 (2013) 333–338

Contents lists available at SciVerse ScienceDirect

Journal of Luminescence

journal homepage: www.elsevier.com/locate/jlumin

Synthesis and luminescence properties of a novel $Na_6CaP_2O_9:Sm^{3+}$ phosphor

G.R. Dillip [a], P. Mohan Kumar [b], B. Deva Prasad Raju [c,a], S.J. Dhoble [d,*]

[a] Department of Physics, Sri Venkateswara University, Tirupati 517 502, India
[b] Department of Physics, K.S. School of Engineering and Management, Bangalore 560 062, India
[c] Department of Future Studies, Sri Venkateswara University, Tirupati 517 502, India
[d] Department of Physics, RTM Nagpur University, Nagpur 440 033, India

ARTICLE INFO

Article history:
Received 23 April 2012
Received in revised form
2 August 2012
Accepted 17 August 2012
Available online 27 August 2012

Keywords:
Inorganic phosphor
Blue-red component
SEM
light emitting diodes

ABSTRACT

Trivalent samarium doped red phosphors $Na_6CaP_2O_9$ were prepared for the first time via high temperature solid state reaction method at 1000 °C. The obtained powders were structurally characterized by X-ray diffraction (XRD), Scanning electron microscopy (SEM) and Fourier transform infrared (FTIR) analyses. The thermal and photo-luminescent properties were also investigated. The calculated Commission International de l'Eclairage (CIE) chromaticity coordinates of the Sm^{3+} ions doped $Na_6CaP_2O_9$ lie in the region of white light. The host matrix has shown a strong blue emission when excited with 403 nm, which has its maximum intensity centered at 475 nm. Red fluorescence originating from intra 4 f $^4G_{5/2} \rightarrow {}^6H_{7/2}$ transition of Sm^{3+} is observed by introducing Sm^{3+} ions into the host lattices of $Na_6CaP_2O_9$ phosphors. The possible energy transfer mechanism from the host to Sm^{3+} ions are analyzed by diffuse reflectance spectroscopy (DRS) analysis. These results suggesting that the $Na_6CaP_2O_9:Sm^{3+}$ phosphors may be a promising blue/red component for cost-effective near UV white light emitting diodes (NUV W-LEDs).

1. Introduction

Over the past few decades, the phosphor research is enormously significant emerging technological field to meet the development of different display and luminescent devices such as solid-state lasers, color TV monitors, fluorescent lamps, lighting, imaging, illuminations, cathode ray tubes, field emission displays, plasma displays, and white light emitting diodes (W-LEDs) [1–3]. In recent years, much attention has been paid to the white LEDs on account of their advantages such as high efficiency, low power consumption, lack of toxic mercury, long lifetime, fast response, energy saving, and environment friendliness. Owing to their excellent properties, white LEDs are considered as the third generation (3G) lighting sources in solid-state lighting system [4–7]. To obtain the white light in solid-state lightening system, there are many methods. One method is by either mixing red, green and blue (RGB) LEDs or by phosphor conversion, in which the light is generated by coating a blue/near UV LED with a yellow or multi-chromatic phosphor. Although, W-LEDs that adopt this kind of white light blending method has been used for many years, some serious problems still exist, such as halo effect due to the different characteristic of LEDs, its poor color rendering index (CRI), narrow visible range and high color temperature caused by lack of red component in the spectra [8,9]. To overcome these problems, another approach to produce the high color rending index and color reducibility for white light is by combining near UV LED (370–410 nm) with RGB phosphors. A suitable red-emitting phosphor for near-UV phosphor converted LEDs should have many potential applications, due to their excellent color rendering index, high color tolerance and high conversion efficiency into visible light [10]. Therefore, it is urgent to find new red phosphors that can be excited by NUV-LED chips for the fabrication of white LEDs.

Rare earth ions in inorganic host matrices form an important class of phosphors as they possess a few interesting characteristics such as excellent chemical stability, high luminescence efficiency, and flexible emission colors with different activators. Further, the f-f transition absorption and emission of the crystalline host activated by rare earths ions are of great importance due to their applications as luminescent optical materials emitting in the visible and near IR regions [11–13]. The selection of the rare earth ion as an activator is a key factor for the preparation of luminescence materials. Among the different rare earth ions, the Sm^{3+} ion as an activator is regarded as one of the most popular and efficient doping ions, which can produces intense orange light in the visible wavelength range. Sm^{3+} ions in various hosts show bright emission in orange or red regions because of the transitions from the excited state $^4G_{5/2}$ to the ground state $^6H_{7/2}$ and also to the higher levels ^6H_j (j=7/2, 9/2, and 11/2) and found the application in high density optical storage, temperature sensors,

---

* Corresponding author.
E-mail address: sjdhoble@rediffmail.com (S.J. Dhoble).

0022-2313/$ - see front matter © 2012 Elsevier B.V. All rights reserved.
http://dx.doi.org/10.1016/j.jlumin.2012.08.025

undersea communications, various fluorescent devices, color display and visible solid-state lasers [14,15].

Selection of suitable host material is also an important factor for the preparation of luminescent materials for different applications. It is well known fact that, phosphor host materials are generally based on borates, phosphates, aluminates, silicates, molybdates, vanadates etc. Among the several inorganic host materials, the phosphate host matrix constitutes as one of the most important luminescence materials, which can produce plenty of crystal field environments imposed on emission contents [16,17]. Rare earth element doped phosphates exhibit strong covalent interaction and high stability strong visible luminescence. In addition, these phosphates have low synthesis temperature and high physical and chemical stability, which makes it as a suitable host lattice for luminescence materials. Luminescence of rare earth ions in phosphates have been widely studied in the past [18–20].

On realizing the relevance and importance of these rare earth ions doped phosphate based phosphors, the present investigation is carried out by the authors. We have been synthesized undoped and Sm^{3+} ions doped $Na_6CaP_2O_9$ host matrix by a conventional high temperature solid state reaction method in air atmosphere. As far as our knowledge is concerned, the Sm^{3+} doped $Na_6CaP_2O_9$ host matrix has not been reported so far. In addition, its structural, thermal, morphological and photoluminescence properties were systematically studied and also analyzed.

2. Experimental

2.1. Synthesis

Undoped and Sm^{3+} ions doped phosphors were prepared by a conventional high temperature solid state reaction method by sintering the samples at 1000 °C in air atmosphere. The starting materials were Na_2CO_3, $CaCO_3$, $NH_4H_2PO_4$ and Sm_2O_3 of high purity analytical reagent grade chemicals and were purchased from Merck, India. The appropriate stoichiometric ratios of these materials were grounded thoroughly in an agate mortar to obtain the homogeneous mixture. Finally, the mixture was kept in a porcelain crucible and sintered at 1000 °C for 4 h in air atmosphere. The obtained products were taken into different studies.

2.2. Characterization

Structural characterization of the prepared phosphors has been carried out from the X-ray diffraction measurements on a Siemens X-ray difractrometer AXS D 5005 with Cu Kα radiation ($\lambda=1.5406$ Å) at 40 kV and 20 mA. The 2θ range was varied between 10° and 80°. An FTIR spectrum was recorded on a Perkin Elmer spectrophotometer with KBr pellet technique in the range 4000–450 cm^{-1}. The surface morphology of the powder phosphor was characterized by scanning electron microscopy (Quanta 200 ESEM). The elemental analysis has been carried out by energy dispersive spectroscopy (EDS) using an X-ray detector attached to the SEM instrument. The differential scanning calorimetry (DSC) analysis of $Na_6CaP_2O_9$ phosphor was carried out in the temperature range from 30 to 450 °C at a heating rate of 10 °C/min under the nitrogen atmosphere using Mettler Toledo DSC 1. Diffuse reflectance spectroscopy (DRS) on synthesized powders was measured using V-670 UV–vis-NIR spectrophotometer (JASCO, Japan). Both the excitation and emission spectra were recorded on a Jobin Vyon Fluorolog −3 fluorescence spectrophotometer equipped with a Xenon lamp as the excitation source. All the measurements were recorded at room temperature.

3. Results and discussion

In order to identify structure and phase purity of the synthesized samples, the powder X-ray analysis was carried out. The XRD patterns of undoped and Sm^{3+} doped $Na_6CaP_2O_9$ powder phosphors sintered at 1000 °C for 4 h are shown in Fig. 1. It reveals that the XRD patterns of $Na_6CaP_2O_9$ phosphor samples with different amounts of rare earth ions are in good agreement with the Joint Committee on Powder Diffraction Standards (JCPDS) data (Card No: 21–1108). It is evidenced from the XRD pattern that there are no Sm_2O_3 peaks in the diffractogram indicating that the added Sm^{3+} ions were incorporated into the $Na_6CaP_2O_9$ lattice. These rare earth ions of small amount did not yield different phase. That is, the Sm^{3+} ions have not caused any significant change after doped into the host lattice structure. The $Na_6CaP_2O_9$ was reported to crystallite in a hexagonal structure with lattice parameters $a=b=12.06$ Å and $c=18.85$ Å [21].

Literature overviews on the maximum value of acceptable percentage difference in ionic radii between doped and substituted cations are 30% [22]. Generally, it is expected that the trivalent samarium (Sm^{3+}) ions occupy the possible cations (Ca^{2+} and P^{5+}) ions in the host lattice, due to the ionic radii of Ca^{2+} ($r_{Ca^{2+}}$), P^{5+} ($r_{P^{5+}}$) and Sm^{3+} ($r_{Sm^{3+}}$) for eight coordinated sites are 112, 17 and 110 pm, respectively [23–25]. The radius percentage difference (D_r) between the doped and substituted ions was estimated based on the following equation, $D_r=100\times[R_m\,(CN)-R_d\,(CN)]/R_m\,(CN)$, where CN is the coordination number, R_m (CN) the radius of the host cation, and R_d (CN) the radius of the doped ion. The calculated values of D_r between Sm^{3+} and Ca^{2+} on eight coordinated sites was found to be 1.78%, while the value of D_r between Sm^{3+} and P^{5+} is −547.05. On the basis of above discussion and the similar ionic radius of cations, it is interpreted that, the doped Sm^{3+} ions are supposed to substitute the Ca^{2+} site in the $Na_6CaP_2O_9$ host. Hence, the authors believed that a small charge dislocation in $Na_6CaP_2O_9:Sm^{3+}$ is most probably compensated by Ca^{2+} vacancies (V_{Ca}), as followed by, $3Ca^{2+}\rightarrow 2Sm^{3+}+V_{Ca}$. Thus, the Sm^{3+} ions occupied only one crystallographic site on the host lattice.

A typical FTIR spectrum of 1000 °C sintered $Na_6Ca_{0.98}P_2O_9:Sm_{0.02}$ is shown in Fig. 2. Usually, the IR absorption band of $(PO_4)^{3-}$ has two regions of 1120–940 cm^{-1} and 650–540 cm^{-1}. From the spectrum, it is observed that the phosphate units are characterized by two broad IR absorption bands near 1031 and 546 cm^{-1} are assigned to the

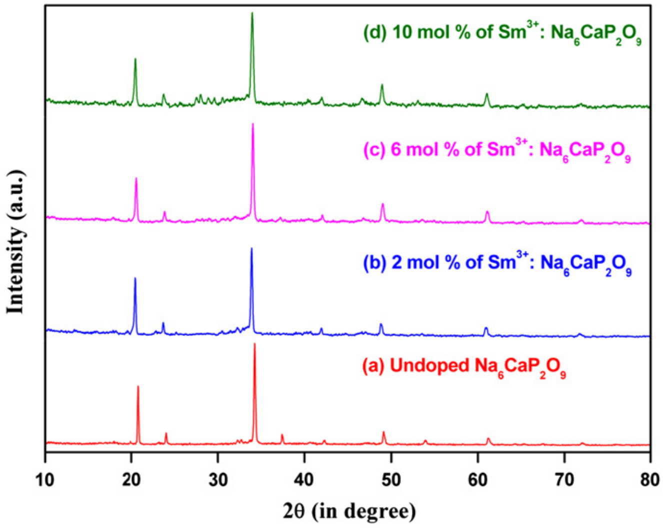

Fig. 1. Powder XRD patterns of undoped and Sm^{3+} ions doped $Na_6CaP_2O_9$ phosphors sintered at 1000 °C.

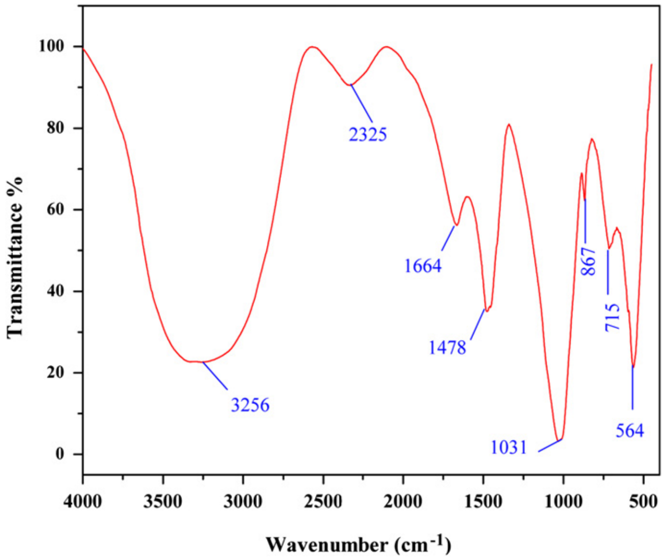

Fig. 2. FT-IR spectrum of $Na_6CaP_2O_9$: Sm^{3+} (2 mol %) powder phosphor.

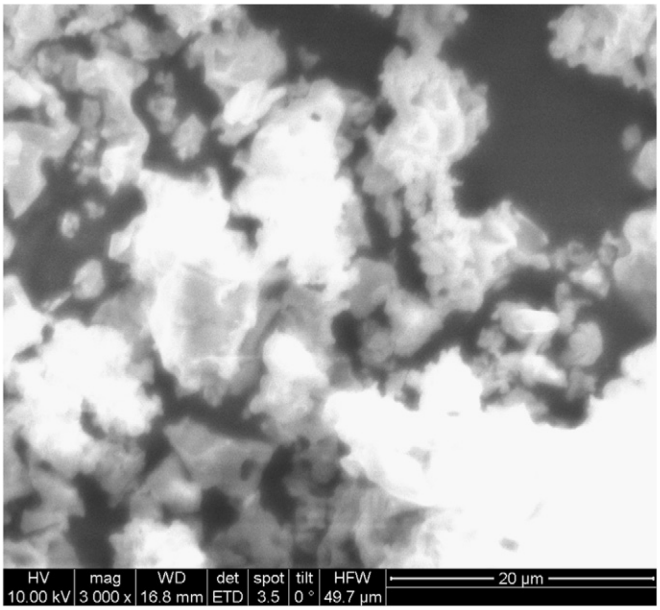

Fig. 3. SEM micrograph of $Na_6CaP_2O_9$: Sm^{3+} (2 mol %) phosphor.

symmetric stretching mode of the $(PO_4)^{3-}$ units. The bands near 3256, 1664 and 1478 cm^{-1} are associated to the OH content, absorbed at the powder surface when the sample was in contact with the environment during the preparation process of measurement [26,27]. A weak band at 2325 cm^{-1} might be due to the C–O vibration of CO_2 in the air. All the assignments made for $Na_6Ca_{0.98}P_2O_9$:$Sm_{0.02}$ phosphor are found to be comparable to the literature reported earlier [28–30].

Fig. 3 shows the SEM image of $Na_6Ca_{0.98}P_2O_9$:$Sm_{0.02}$ powder phosphor. The obtained micrograph shows that the particles are agglomerated and it possess an irregular morphology. However, the actual size of the particles is cannot be determined from the SEM image. From the micrograph, it is clear that the approximate size of the particles might be in micrometer range which is in favor of its application in LEDs. Owing to their high luminescence with the advantage of micrometer dimension, suggest that these phosphors will find more applications in the field of display and lighting [31,32]. To determine the composition of the prepared products, an EDS spectrum is presented in Fig. 4. It is found that the phosphors are composed of Na, Ca, P, O and Sm.

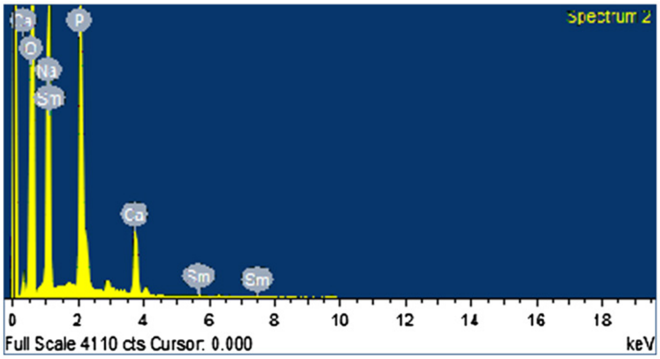

Fig. 4. EDS profile of $Na_6CaP_2O_9$: Sm^{3+} (2 mol%) phosphor.

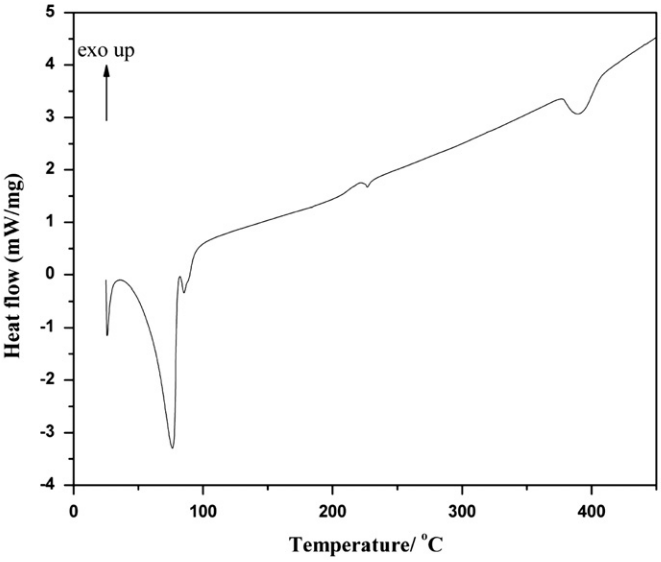

Fig. 5. DSC curve of $Na_6CaP_2O_9$: Sm^{3+} (2 mol %) phosphor.

The obtained DSC profile is shown in Fig. 5. The obvious endothermic peaks in the region 30–100 °C are to the evaporation of free and adsorbed water and the weak endothermic peak at 227 °C is attributed to the decomposition of NH_3. The endothermic peak at around 390 °C is accompanied by the removal of CO_2 gases that occurs from the starting materials [33].

In order to investigate the energy absorption of undoped and Sm^{3+} ions doped $Na_6CaP_2O_9$ phosphors, the DRS spectra was recorded and is shown in Fig. 6. The spectra shows a strong absorption band in the shorter wavelength range 230–280 nm (i.e. higher energy) for all samples may be ascribed to the absorption of the host lattice. When Sm^{3+} ions is introduced into the host lattices, several weak absorption bands in the larger wavelength range 345–480 nm (i.e. low energy) are observed. These electronic bands are the characteristics of Sm^{3+} ions, starting from ground state $^6H_{5/2}$ to the various excited states of Sm^{3+} ions. These transitions are identified at 345, 362, 377, 405, 421, 440, 464 and 478 nm corresponds to $^6H_{5/2}\rightarrow{}^4K_{17/2}$, $^6H_{5/2}\rightarrow{}^4H_{7/2}$, $^6H_{5/2}\rightarrow{}^6P_{7/2}$, $^6H_{5/2}\rightarrow{}^6F_{7/2}$, $^6H_{5/2}\rightarrow{}^6P_{5/2}$, $^6H_{5/2}\rightarrow{}^4G_{9/2}$, $^6H_{5/2}\rightarrow{}^4I_{9/2}$ and $^6H_{5/2}\rightarrow{}^4I_{11/2}$, respectively [34]. These bands are also evident from the excitation spectrum (Fig. 7). The reports on the charge transfer band (CTB) of Sm^{3+} ions were appeared in the literature. For instance, Liang et al. [35] prepared the rare earth ions doped strontium orthophosphate and they were found the CTB of Sm^{3+} ions at 206 nm. Chen and co-workers [36] reported that the

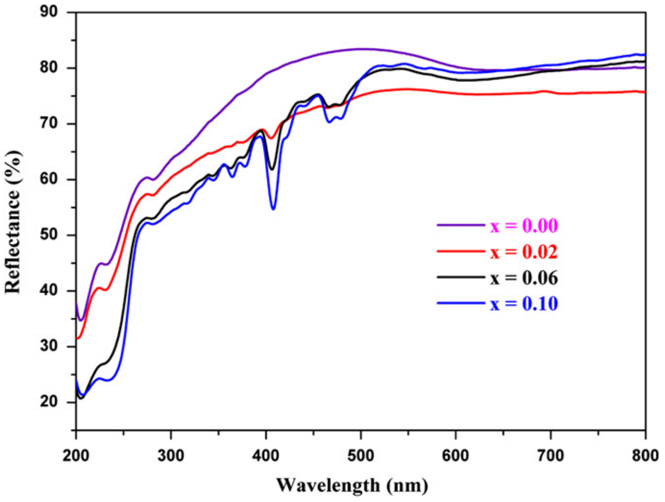

Fig. 6. The diffuse reflection spectra of $Na_6Ca_{1-x}P_2O_9$:Sm_x (x=0.00–0.10).

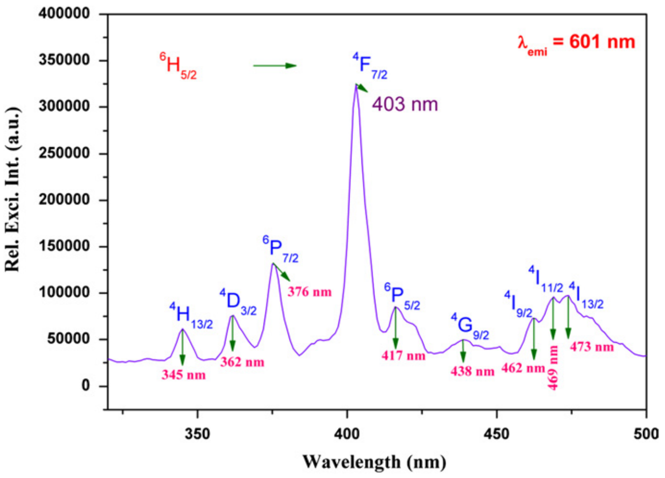

Fig. 7. Excitation spectrum of $Na_6CaP_2O_9$: Sm^{3+} (2 mol %) phosphor.

CTB was observed in the region 260–310 nm of Sm^{3+} ions doped $NaGd(WO_4)_2$ phosphors. In our present investigation, we obtained the CTB of Sm^{3+} ions at 231 nm, which is consistent with the earlier reports. The observed largest absorption band near 405 nm is corresponding to the transition from the $^6H_{5/2}$ ground level to the $^4F_{7/2}$ excited levels, which is in consistent with the excitation spectra. Due to the increasing Sm^{3+} ion concentration, the absorption bands of Sm^{3+} ions are becoming stronger. Hence, it implies that there is an efficient energy transfer from the host matrix to Sm^{3+} ions. The increasing Sm^{3+} concentration accompanies enhancement of the absorption and also these edges are seen to be shifted towards the higher wavelengths region (i.e. lower energies), indicating the incorporation of Sm^{3+} ions in the host lattice. This is due to the slight variation in the radii of the doped Sm^{3+} ions and host cations (Ca^{2+}), which is consistent with the XRD results. Therefore, it is clear that the Sm^{3+} ions create localized energy levels with the electronic structure of the host material, furnishing an efficient absorption pathway for visible light.

Fig. 7 shows the excitation spectrum of $Na_6Ca_{0.98}P_2O_9$:$Sm_{0.02}$ powder phosphor sintered at 1000 °C. In the wavelength region 320–550 nm, several excitation peaks are observed and are located at 345 nm ($^6H_{5/2}\rightarrow{}^6H_{13/2}$), 362 nm ($^6H_{5/2}\rightarrow{}^4D_{3/2}$), 376 nm ($^6H_{5/2}\rightarrow{}^6P_{7/2}$), 403 nm ($^6H_{5/2}\rightarrow{}^4F_{7/2}$), 417 nm ($^6H_{5/2}\rightarrow{}^6P_{5/2}$), 438 nm ($^6H_{5/2}\rightarrow{}^4G_{9/2}$), 462 nm ($^6H_{5/2}\rightarrow{}^4I_{9/2}$), 469 nm ($^6H_{5/2}\rightarrow{}^4I_{11/2}$) and 473 nm ($^6H_{5/2}\rightarrow{}^4I_{13/2}$) which are attributed to f–f transitions of Sm^{3+} charge transfer band of Sm^{3+}–O^{2-} interaction [37,38]. From the excitation spectrum, it was found that the intensity of f–f transition at 403 nm is high compared with the other transitions and has been chosen for the measurement of emission spectra of Sm^{3+}:$Na_6CaP_2O_9$ phosphors. The most intense peak at 403 nm clearly indicates that these phosphors are effectively excited by near ultraviolet light emitting diodes.

Fig. 8 reveals that the emission spectra of undoped and Sm^{3+} ions doped $Na_6CaP_2O_9$ phosphors with an excitation wavelength of 403 nm. The emission spectra consist of two parts: one is a broad band from 425 to 550 nm may be attributed to the host emission, which is peaking at 475 nm, another region comprising three sharp emission lines from 550 to 670 nm are the characteristic of the samarium ions. Three peaks are ascribed to the $^4G_{5/2}\rightarrow{}^6H_{5/2}$, $^4G_{5/2}\rightarrow{}^6H_{7/2}$ and $^4G_{5/2}\rightarrow{}^6H_{9/2}$ transitions at 565, 601 and 646 nm of the Sm^{3+} ions, respectively. Among these, the transition at 601 nm ($^4G_{5/2}\rightarrow{}^6H_{7/2}$) is having the maximum intensity, which corresponds to the red emission of Sm^{3+}:$Na_6CaP_2O_9$ phosphors. It can be stated that the strong red emitting transition $^4G_{5/2}\rightarrow{}^6H_{7/2}$ at 601 nm ($\Delta J=\pm 1$) is a partly magnetic dipole (MD) and partly electric dipole (ED) nature emission band. The other transition at 565 nm ($^4G_{5/2}\rightarrow{}^6H_{5/2}$) is purely MD natured and at 646 nm ($^4G_{5/2}\rightarrow{}^6H_{9/2}$) is purely ED natured, which is sensitive to crystal field. Generally, the intensity ratio of ED and MD transition has been used to measure the symmetry of the local environment of the trivalent 4f ions [39]. The greater the intensity of the ED transition, the more the asymmetry nature. In our present study, the $^4G_{5/2}\rightarrow{}^6H_{5/2}$ (MD) transition of Sm^{3+} ions is more intense than $^4G_{5/2}\rightarrow{}^6H_{9/2}$ (ED) transition, indicating the symmetric nature of the $Na_6CaP_2O_9$ host matrix.

Literature overviews on the energy transfer mechanism from host to lanthanide (Ln^{3+}) ions doped phosphors have appeared [40–43]. For instance, Lei and co-workers [44] prepared a series of Sm^{3+} ions doped long-lasting $CdSiO_3$ phosphors that gave a host emission at 400 nm with an excitation wavelength of 254 nm. Rosa-Cruz [45] et al. observed a blue emission band for Sm^{3+} activated ZrO_2 phosphors at 490 nm under excitation at 320 nm. Vengal Rao [46] et al. synthesized host sensitized $CaZrSi_2O_7$ red phosphor incorporated with Eu^{3+}, which yields a blue emission peaking at 470 nm under excitation at 290 nm. In our present investigation, in the region 425–550 nm, we noticed a single broad emission band centered at 475 nm from host lattices upon the excitation wavelength of 403 nm. This blue emission can be

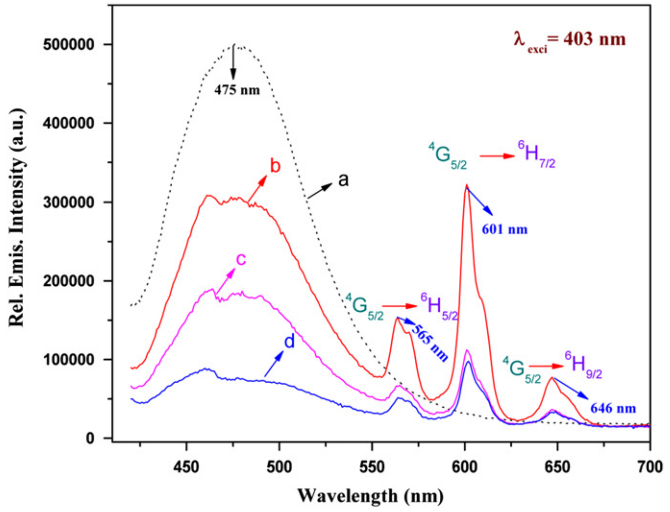

Fig. 8. Emission spectra of (a) Undoped $Na_6CaP_2O_9$ (b) 2 mol% of Sm^{3+} (c) 6 mol % of Sm^{3+} and (d) 10 mol% of Sm^{3+} with an excitation wavelength of 403 nm.

produced by the radiative recombination of a localized electron in the donor band with a trapped hole [47]. First of all, the authors studied the emission spectra of $Na_6CaP_2O_9$:Sm^{3+} phosphors with 2 mol % of Sm^{3+} ion concentration. On the careful observation, the broad emission of the undoped samples overlap the samarium excitation bands, this fact suggest an efficient energy transfer has occurred from host lattices (donor) to the dopant Sm^{3+} (acceptor).

We assume that when Sm^{3+} is present in host lattices, this missed energy can be non-radiatively transferred to the dopant, resulting in its characteristic emission band of this active ion. It is well known fact that the luminescence performance of the powder phosphors depends mainly on the concentration of activator ions, thus the identification of optimum dopant concentration is necessary [48]. In order to optimize dopant concentration, we varied Sm^{3+} ions concentration in the host $Na_6CaP_2O_9$. Fig. 9 shows the dominant fluorescence emission intensity of Sm^{3+} as a function of its activator concentration in $Na_6CaP_2O_9$: Sm^{3+} phosphors. It is clear from spectrum that the increase of the Sm^{3+} ions concentration decreases the blue emission of host lattices, indicating the possible energy transfer from host to Samarium. Unfortunately, the dominant intensity of Sm^{3+} ions at 601 nm is also quenched and is shown in Fig. 8. Blasse [49] et al. proposed that at higher concentration, the cluster formation increases due to ion interaction and leading to quenching of the Sm^{3+} fluorescence. Hence, the 2 mol % of Sm^{3+} ions is the optimum dopant concentration.

In the present investigation, it is observed from PL spectra that the intensity of fluorescence emission of host (undoped $Na_6CaP_2O_9$) at 475 nm is higher than that of the fluorescence emission of Sm^{3+} ions at 601 nm. An important finding of our present work is that we observed blue/red light phosphorescence in Sm^{3+} activated $Na_6CaP_2O_9$ phosphors. Hence, it might be useful in W-LEDs, CRT, flat panel displays, etc.

The chromaticity diagram established by the Commission International de l'Eclairage (CIE) in 1931 is a two dimensional graphical representation of any color perceivable by the human eye on an *x*–*y* plot. Fig. 10 depicts the chromaticity coordinates of $Na_6CaP_2O_9$:Sm^{3+} (2, 6 and 10 mol %) phosphors sintered in air atmosphere under the excitation of 403 nm. This indicates that the color coordinates are located in the near white region for prepared phosphors and these phosphors might be useful in the fabrication of NUV W-LEDs.

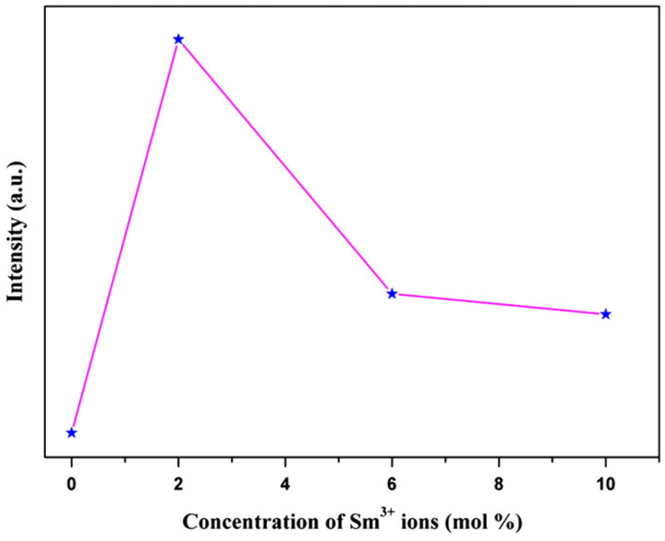

Fig. 9. The variation of PL intensity with Sm^{3+} ion concentration.

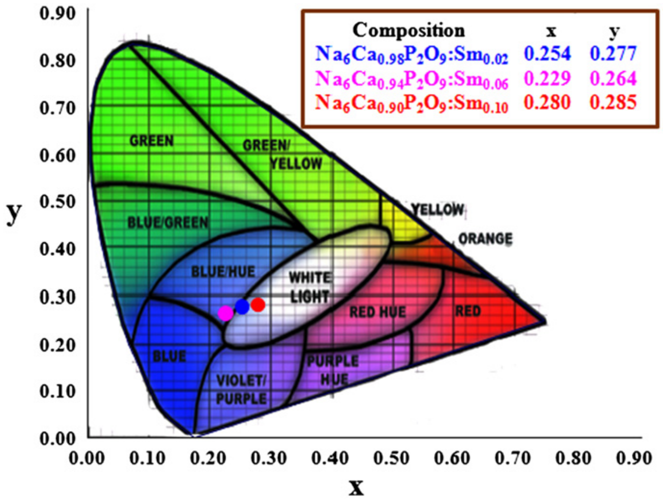

Fig. 10. CIE color coordinates of $Na_6CaP_2O_9$: Sm^{3+} (2, 6 and 10 mol %) phosphors.

4. Conclusions

In conclusion, the strong host sensitized novel red phosphor $Na_6CaP_2O_9$:Sm^{3+} (Sm^{3+} = 0, 2, 6 and 10 mol %) has been successfully prepared by the conventional solid state reaction method at 1000 °C in air atmosphere. XRD analysis indicated the hexagonal structure of the prepared phosphors. The elemental composition is verified with EDS analysis and DSC analysis has been carried out to study the thermal properties. The efficient energy transfer occurs from the host to Sm^{3+} ions was discussed by DRS. PL results indicated that the prepared phosphors showed strong red emission lines at 601 nm corresponding to the $^4G_{5/2} \rightarrow {}^6H_{7/2}$ transition of Sm^{3+} ions. This resulting efficient host to Sm^{3+} sensitization and micrometer in size may find more applications in display and W-LEDs.

Acknowledgments

The authors are sincerely thankful to XRD facility extended by Dr. C. Shivakumara, Senior Scientific Officer, Solid State and Structural Chemistry Unit and Spectroscopy/Analytical Test Facility (SATF), Indian Institute of Science, Bangalore and Sophisticated Analytical Instrumentation Facility (SAIF), IIT, Chennai for extending the instrumental facilities. One of the author SJD thanks to UGC, New Delhi for financial assistance during this work.

References

[1] N. Kadama, T. Takahashi, M. Yamaga, Y. Tanii, J. Qin, K. Hirao, Appl. Phys. Lett. 75 (1998) 7202.
[2] W. Chen, J.O. Bovin, A.G. Joly, S. Wang, F. Su, G. Li, J. Phys. Chem. B. 108 (2004) 11927.
[3] T. Chen, Z. Zhou, Y. Wang, Sens. Actuat. B: Chem. 143 (2009) 124.
[4] J.S. Kim, P.E. Jeon, Y.H. Park, J.C. Choi, H.L. Park, G.C. Kim, T.W. Kim, Appl. Phys. Lett. 85 (2004) 3696.
[5] S. Sailaja, S.J. Dhoble, N. Brahme, B.S. Reddy, J. Mater. Sci. 46 (2011) 7793.
[6] G. Ju, Y. Hu, L. Chen, X. Wang, Z. Mu, H. Wu, F. Kang, Opt. Laser Tech. 44 (2012) 39.
[7] A. Tang, D.F. Zhang, L. Yang, J. Lumin. 132 (2012) 1489.
[8] S. Nakamura, G. Fasal, The Blue Laser Diode, Springer, Berlin, 1997.
[9] D.K. Yim, I.S. Cho, C.W. Lee, J.H. Noh, H.S. Roh, K.S. Hong, Opt. Mater. 33 (2011) 1036.
[10] S. Ye, F. Xiao, Y.X. Pan, Y.Y. Ma, Q.Y. Zhang, Mater. Sci. Eng. R 71 (2010) 1.
[11] M.R. Brown, A.F.J. Cox, W.A. Shand, J.M. Willian, J. Phys. C: Solid State Phys. 5 (1972) 502.
[12] G. Blasse, Chem. Mater. 1 (1989) 294.
[13] E. Song, W. Zhao, G. Zhou, X. Dou, C. Yi, M. Zhou, J. Rare Earths 29 (2011) 440.
[14] Y.L. Li, Y.H. Chang, Y.F. Lin, Y.S. Chang, Y.J. Lin, J. Alloys Comp. 439 (2007) 367.

[15] A.A. Setlur, J.J. Shiang, U. Happek, Appl. Phys. Lett. 92 (2008) 081104.
[16] T.J. Xie, N. Hirosaki, Sci. Technol. Adv. Mater. 8 (2007) 588.
[17] Y.S. Tang, S.F. Hu, C.C. Lin, N.C. Bagkar, R.S. Liu, Appl. Phys. Lett. 90 (2007) 151108.
[18] M. Ferhi, K. Horchani-Naifer, M. Ferid, J. Rare Earths 27 (2009) 182.
[19] C. Qin, Y. Huang, L. Shi, G. Chen, X. Qiao, H.J. Seo, J. Phys. D: Appl. Phys. 42 (2009) 185105.
[20] L. Shi, Y. Huang, H.J. Seo, J. Phys. Chem. A 114 (2010) 6927.
[21] Znamicrowska Berak, Rocz. Chem. 41 (1967) 2065.
[22] A.M. Pires, M.R. Davolos, Chem. Mater. 13 (2001) 21.
[23] P.L. Li, Z.J. Wang, Z.P. Yang, Q.L. Guo, Chin. Phys. Lett. 28 (2011) 017801.
[24] W. Li, M. Wang, Z.H. Li, X.F. Shang, H. Wang, Y.W. Wang, Y.B. Xu, Russ. J. Electrochem. 43 (2007) 1279.
[25] H.N. Luitel, T. Watari, T. Chand, T. Torikai, M. Yada, Opt. Mater. 34 (2012) 1375.
[26] R.A. Nyquist, R.O. Kagel, Infrared Spectra of Inorganic Compounds (3800–45 cm−1), Academic Press, NY, 1992, P. 232.
[27] Y. Huang, X. Wang, H.S. Lee, E. Cho, K. Jang, Y. Tao, J. Phys. D: Appl. Phys. 40 (2007) 7821.
[28] F. Lei, B. Yan, J. Solid State Chem. 181 (2008) 855.
[29] B. Yue, J. Gu, G. Yin, Z. Huang, X. Liao, Y. Yao, Y. Kang, P. You, Current Appl. Phys. 10 (2010) 1216.
[30] B.K. Grandhe, V.R. Bandi, K. Jang, S.S. Kim, D.S. Shin, Y.I. Lee, J.M. Lim, T. Song, J. Alloys Comp. 509 (2011) 7937.
[31] B. Yan, C. Wang, Solid State Sci. 10 (2008) 82.
[32] V.R. Bandi, B.K. Grandhe, M. Jayasimhadri, K. Jang, H.S. Lee, S.S. Yi, J.H. Jeong, J. Crystal Growth 326 (2011) 120.
[33] B. Wong, L. Sun, H. Ju, J. Sol-Gel Sci. Technol. 53 (2010) 454.
[34] Z. Xia, D. Chen, J. Am. Ceram. Soc. 93 (2010) 1397.
[35] H. Liang, Y. Tao, Q. Su, S. Wang, J. Solid State Chem. 167 (2002) 435.
[36] Y. Chen, H.K. Yang, J.W. Chung, B.K. Moon, H. Choi, J.H. Jeong, J. Korean Physical Soc. 57 (2010) 1760.
[37] A. Newport, J. Silver, A. Vecht, J. Electrochem. Soc. 147 (2002) 3944.
[38] B. Lei, Y. Liu, G. Tang, Z. Ye, C. Shi, Mater. Chem. Phys. 87 (2004) 227.
[39] Z. Wang, P. Li, Z. Yang, Q. Guo, J. Lumin. 132 (2010) 1944.
[40] A. Kudo, Chem. Mater. 9 (1997) 664.
[41] B.L. An, M.L. Gi, M.X. Li, J.M. Zhang, J. Mol. Struct. 687 (2004) 1.
[42] W. Leo, R. Li, X. Chen, J. Phys. Chem. C 113 (2009) 8772.
[43] Y. Hen, J. Wang, C. Lin, X. Kuang, Q. Su, Appl. Phys. Lett. 98 (2011) 081917.
[44] B. Lei, Y. Liu, J. Liu, Z. Ye, C. Shi, J. Solid State Chem. 177 (2004) 1333.
[45] E.D.L. Rosa-Cruz, L.A. Diaz-Torres, P. Salas, R.A. Rodriguez, G.A. Kumar, M.A. Meneses, J.F. Mosino, J.M. Hernandez, O. Barbosa-Garcia, J. Appl. Phys. 94 (2003) 3509.
[46] V.R. Bandi, M. Jayasimhadri, J. Jeong, K. Jang, H.S. Lee, S.S. Yi, J.H. Jeong, J. Phys. D: Appl. Phys. 43 (2010) 395103.
[47] J. Palm, F. Gan, B. Zheng, J. Michel, L.C. Kimerling, Phys. Rev. B 54 (1996) 17603.
[48] S. Sailaja, S.J. Dhoble, B.S. Reddy, J. Mol. Struct. 1003 (2011) 115.
[49] P.A.M. Berdowski, G. Blasse, J. Solid State Chem. 63 (1986) 86.